Title

A Simplified Low-${Q}$ Electrically Small Magnetic Dipole Antenna

Authors

Madsen, Kristian N
Zhou, Yunshun
Sievenpiper, Daniel F

Publication Date

2016

DOI

10.1109/lawp.2016.2546941

Peer reviewed

A Simplified Low-Q Electrically Small Magnetic Dipole Antenna

Kristian N. Madsen, *Member, IEEE*, Yunshun Zhou, and Daniel F. Sievenpiper, *Fellow, IEEE*

***Abstract*—An electrically small wire cage antenna is presented as an alternative to previously proposed spherical split-ring (SSR) antennas, which achieve Q's near the lower limit defined by Chu. This design is targeted to approach the same lower bound, but constructed in a manner more economical for production. The proposed dual-polarized wire cage structure is produced using a standard dielectric substrate which is patterned front and back with copper, using well-defined and reproducible etching procedures. The thin interdigitated structure is then placed over a ground plane using rigid conducting elements that help to suspend the dielectric substrate while completing the wire cage. A parameterized HFSS model was used to optimize performance. Measurements were made on fabricated prototypes that demonstrate performance consistent with simulated results, confirming that SSR antennas and their derivatives are capable of approaching Chu's limit on the radiation efficiency of electrically small antennas.**

***Index Terms*—Chu limit, electrically small antenna, magnetic dipole antenna, spherical split ring, wire cage antenna.**

I. Introduction

THE THEORETICAL limitations linking an antenna's size to its bandwidth and efficiency were derived by Wheeler [1] and Chu [2] in the 1940s and serve as a benchmark for the expected performance of all new antenna designs. Electrically small antennas find use in applications where the size of the antenna must be minimized at the cost of bandwidth or efficiency. Generally, the designs that fare best have aspect ratios near unity [3] and show a uniformity in the distribution of fields surrounding the antenna. Newly developed electrically small magnetic dipole antennas demonstrate radiation Q's near the lower limit defined by Chu. This letter attempts to maximize both bandwidth and efficiency by following the design methodologies presented in previous works, while using more favorable manufacturing techniques.

II. Magnetic Dipole Antennas

Magnetic dipole antennas have been explored in a number of forms and configurations as developed in earlier literature. The general concept in these designs is that a time harmonic electrical current is impressed on a spherical surface—or elements approximating a spherical surface—so that the appearance of a magnetic dipole is formed. The Q of magnetic dipole antennas is limited in its value to a lower bound of three times the lower bound ($Q_{\mathrm{MD}} \geq 3Q_{\mathrm{lb}}$) derived by Chu

$$Q_{\mathrm{lb}} = \eta_r \left(\frac{1}{n\,(ka)^3} + \frac{1}{ka} \right) \tag{1}$$

a result derived by Thal [6] and demonstrated experimentally in a number of prior works [4], [7], [8]. Q_{lb} is related to the electrical size of the antenna, ka, where $k = 2\pi/\lambda$ and a is the radius of a sphere that encloses the outer extremities of the antenna. In addition, Q_{lb} is proportional to the radiation efficiency η_r of the antenna, as well as the number of supported resonant modes n. Equation (1) can be manipulated to form

$$B\eta_r\,(\max) = \frac{s-1}{\sqrt{s}} \left(\frac{1}{n\,(ka)^3} + \frac{1}{ka} \right)^{-1} \tag{2}$$

which establishes the maximum bandwidth-efficiency product $B\eta_r\,(\max)$ for an antenna with an electrical dimension smaller than a sphere of radius ka with n resonant modes. The fractional bandwidth B is defined for the range of frequencies where the VSWR remains lower than s.

Electric dipoles have been studied more comprehensively than magnetic dipoles, which might be owed to a number of factors, including their ability to be designed over a ground plane, thus requiring only the construction of a monopole, and their ability to attain values of Q more closely approaching the Chu limit ($Q_{\mathrm{ED}} \geq 1.5\ Q_{\mathrm{lb}}$). Fano *et al.* [9] describe a magnetic dipole produced by a surface current directed in ϕ with a density proportional to $\sin\theta$. Although a specific design is not described explicitly in the Fano text, this concept is advanced by Best [7], who envisions a magnetic dipole that is simply the complement of the electric dipoles presented in his earlier work [10], [11]. His magnetic dipole is capable of approaching the Chu limit and shows promising efficiency in some configurations. In addition, some of his designs were capable of achieving resonant resistances near 50 Ω, which overcame previous limitations of electrically small magnetic dipoles.

The work by Best is further expanded upon by Kim, first in the form of a multiarm spherical helix (MSH) [5] and then as a spherical split ring (SSR) [4], which for all intents and purposes apply the same principles as Fano *et al.*, while simplifying the geometry of the structure needed to generate the $\sin\theta$ weighted currents. Kim's SSR design shown in Fig. 1(a) forms a resonator using a series of wire rings distributed evenly in θ. Neighboring rings are flipped with respect to one another, and a ground plane is used to generate an illusionary spherical current distribution. This design operates as a conventional

Manuscript received April 1, 2015; revised March 11, 2016; accepted March 22, 2016. Date of publication March 25, 2016; date of current version December 20, 2016.

The authors are with the Electrical and Computer Engineering, University of California, San Diego, San Diego, CA 92103 USA (e-mail: kristiannm@hotmail.com; shunshunz19@gmail.com; dsievenpiper@eng.ucsd.edu).

Color versions of one or more of the figures in this letter are available online at http://ieeexplore.ieee.org.

Digital Object Identifier 10.1109/LAWP.2016.2546941

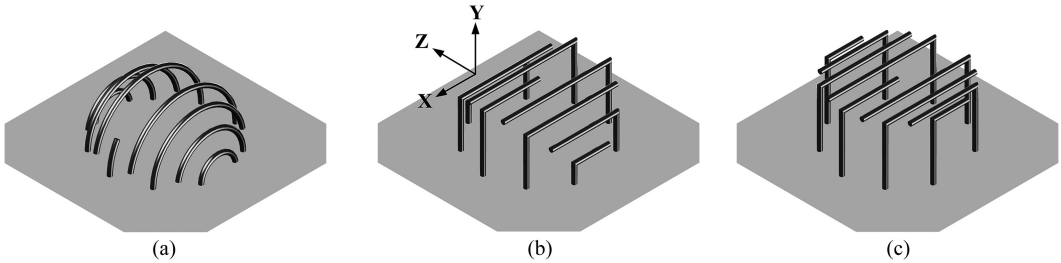

Fig. 1. Various SSR structures. (a) Design proposed by Kim [4]. (b) L-shaped elements distributed evenly in θ. (c) Lateral elements brought into the same plane.

split-ring resonator (SRR) [8]. However, this multielement configuration distributes current more evenly over its surface than a dual- or single-element SRR. The general consensus in these designs is that an antenna that approaches the Chu limit is one that effectively utilizes a spherical volume.

III. Dual-Polarized Wire Cage Antenna

The dual-polarized wire cage (DPWC) antenna is a modification of the SSR antenna that follows the same design methodology but utilizes L-shaped elements to approximate the spherical rings used in Kim's design. The structure of the DPWC can approximate the SSR more closely given a higher degree of complexity, but in the interest of manufacturability, the complexity is reduced; thus, reducing its similarity with the SSR, effectively diminishing the quality of the uniform spherical current distribution and less efficiently utilizing a spherical volume.

Fig. 1(b) and (c) is a simplification of the SSR geometry, easily specified using Cartesian coordinates. Fig. 1(b) simplifies the design by eliminating the curved segments of wire shown in Fig. 1(a) and replacing them with L-shaped elements. This is further simplified in Fig. 1(c), where the lateral segments of the L-shaped elements are brought into the same plane. Moving from spherical to Cartesian coordinates helps to ease the fabrication process. Additionally, the L-shaped nature of the elements allows the lateral portion to be fabricated on a planar dielectric substrate, further simplifying the design.

A. Multiple Mode Operation

Using a rigid dielectric substrate is also advantageous because the L-shaped elements can be patterned perpendicularly to generate orthogonally polarized modes. These copper traces can be adapted with little effect on the other resonance so that the center frequency and match of each mode can be tuned somewhat independently. A rendering of the HFSS model shown in Fig. 2 looks similar to Fig. 1(c) with a second set of lateral elements rotated 90° about the z-axis. A thin semitransparent dielectric is shown in this rendering with lateral (xy-plane) strips of metal patterned on the front and back surfaces. The vertical elements can be constructed from rigid or semirigid conducting material that would screw or solder to the ground plane and top portion of the antenna, linking the two. In this design, the vertical elements are formed by semirigid uninsulated copper wire, drawn through holes in the dielectric material and ground plane and then soldered in place.

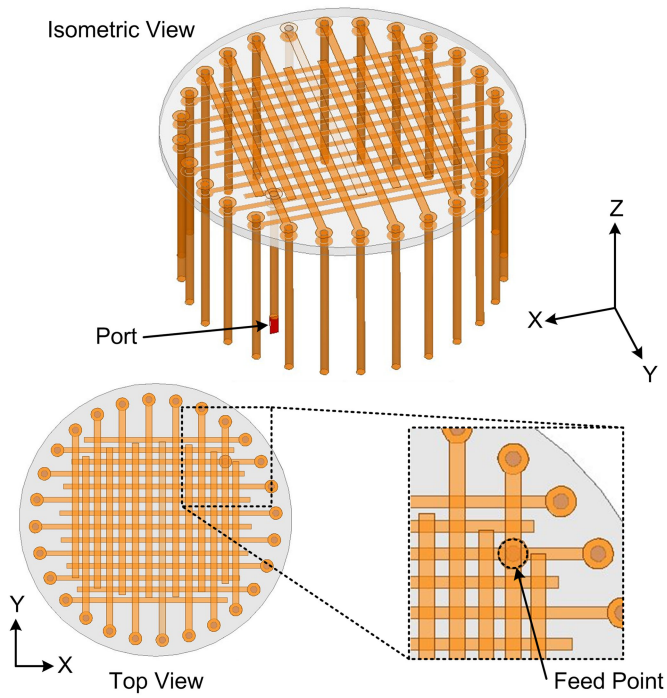

Fig. 2. Wire cage antenna modeled using Ansoft HFSS.

The feed for the wire cage is adapted from the SSR design, breaking the symmetry of the antenna, but allowing for both modes to be excited from the same source. In practice, the vertical feed can be placed anywhere the top and bottom traces overlap. However, special attention must be given when choosing its location, as this will undoubtedly have an effect on radiation resistance and resonant frequency of the antenna. The placement of the feed is highlighted in the inset of Fig. 2, where the feedpoint is made at the intersection of the y-oriented element second from right and the x-oriented element third from top. The selection of this feed location was made to achieve a 50-Ω match, without requiring external matching.

B. Simulation and Parameterized Model

The proposed antenna structure was modeled and simulated using HFSS. The model was parameterized so that optimization simulations could be run over a number of variables specifying the design. As Fig. 2 shows, the model of the circular wire cage is excited near the termination of the feed element and the ground plane (red sheet models 50-Ω port). Fig. 3 shows that

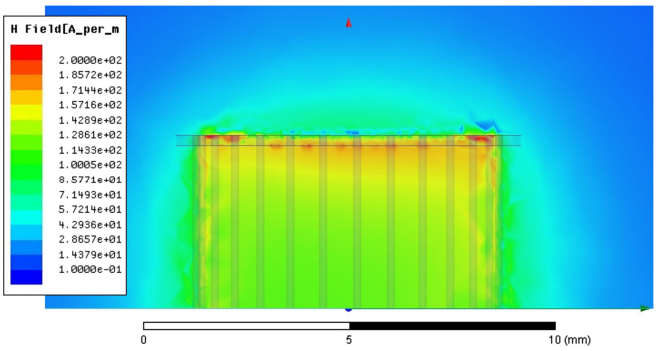

Fig. 3. Magnetic field distribution within the wire cage.

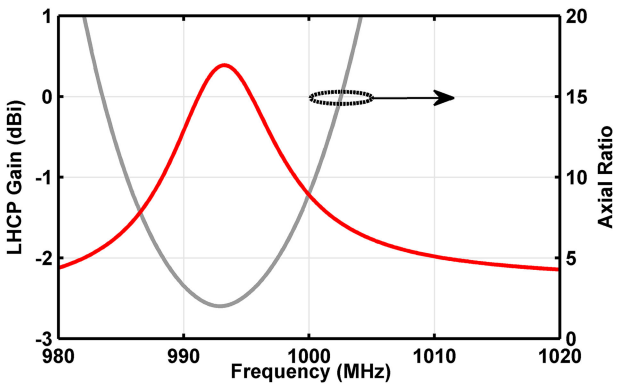

Fig. 4. LHCP gain and axial ratio in the band of interest.

the internal magnetic fields are distributed uniformly within the volume of the antenna, which is shown to be the case for TE-mode resonators [7]. The antenna generates left-hand circularly polarized waves as shown in Fig. 4, where the axial ratio is roughly two near the frequency of peak gain. Perturbation of the top and bottom wire lengths enables tuning of the circular polarized mode and optimization of the axial ratio. Additionally, the polarization can be changed from left-hand circular polarization (LHCP) to right-hand circular polarization (RHCP) through this method of adjustment.

IV. Measurement

Here, results are presented for a fabricated circular DPWC similar to the design shown in Fig. 2. The circular dielectric material that is used to construct the top portion of the wire cage is 20-mil-thick Rogers 4003 ($\varepsilon_r = 3.38$ and $\delta = 0.0027$ at 10 GHz) with a radius of 8.5 mm. The lateral radiating elements are half-ounce copper traces patterned on the surface of the Rogers substrate. The widths of the top and bottom traces are 16 and 12 mil, respectively, and their lengths vary from 1.2 to 1.4 cm depending on their proximity to the center of the circle. The circular substrate is suspended 8 mm above a ground plane using 12-mil bare copper wires. The ground plane is a 15 cm $\times$ 15 cm square of FR4 coated in copper. The feed was formed using the same 12-mil copper wire that contacts the inner conductor of a rigid coaxial cable through a hole in the ground plane. The outer coaxial conductor was soldered to the back side of the ground

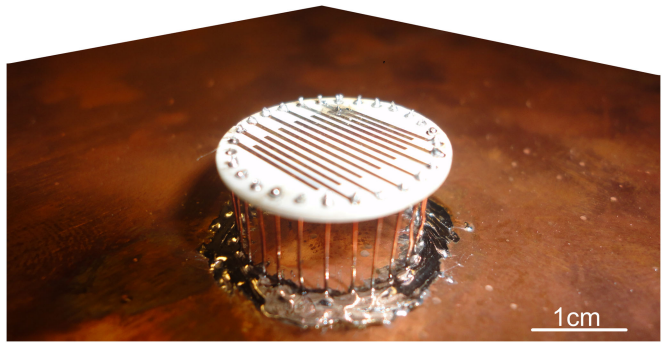

Fig. 5. Simple circular wire cage antenna prototype.

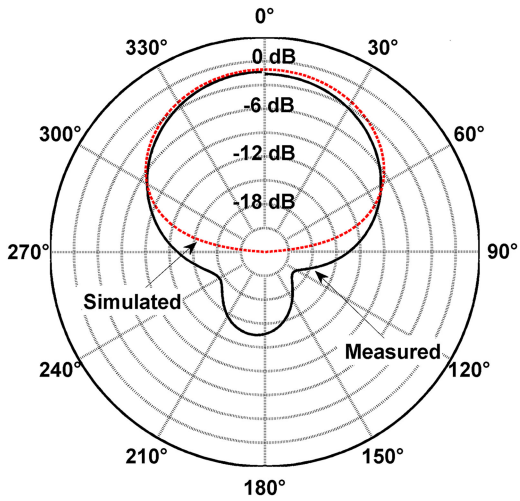

Fig. 6. Antenna gain shown in dBi.

plane. Transmission measurements of the DPWC antenna were made within an anechoic chamber. The antenna was mounted on a rotary stage, with a fixed receive antenna capable of measuring vertical and horizontal polarizations independently.

The prototype circular antenna shown in Fig. 5 is the embodiment of the structure proposed in Fig. 2. As a validation of the ability to model the antenna's performance, Fig. 6 depicts the measured antenna pattern and gain in comparison to the simulation. Additionally, Fig. 7 makes a comparison between the simulated and measured return loss of the antenna, which demonstrate close agreement. The gain and directivity of Fig. 6 are used to determine the efficiency of the antenna as outlined in [3].

The antenna gain (measured normal to ground plane) of both the horizontal and vertical polarized modes is shown as a function of frequency in Fig. 8, which indicates that the antenna has two distinct bands of operation. The efficiency of the antenna was determined at the frequencies corresponding to the peak power transmission of both the horizontal and vertical polarized modes. These efficiencies along with the bandwidth and Q of each mode are tabulated in Table I.

Table I compares the proposed design to published results from several other magnetic dipole antennas. It should be mentioned that the Q/Q_{LB} ratio for the proposed design is below

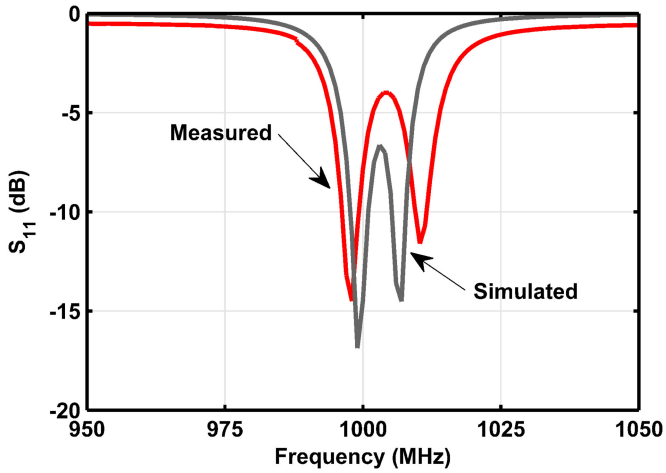

Fig. 7. Comparison of return loss.

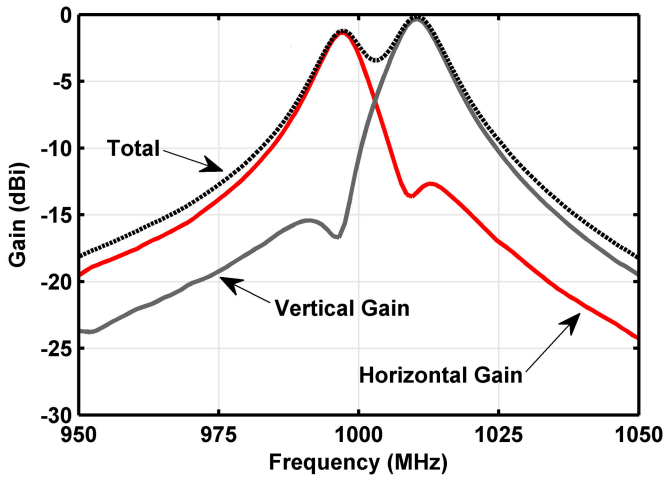

Fig. 8. Measured gain of the horizontal and vertical polarized mode as a function of frequency. Measured normal to the ground plane.

TABLE I
WIRE CAGE ANTENNA PERFORMANCE SUMMARY

Design	[7]	[4]	This Work
Resonant Frequency	306.4 MHz	403 MHz	1004 MHz
Bandwidth	2.06 MHz	0.90 MHz	23.5 MHz
Fractional Bandwidth	0.67%	0.22%	2.33%
ka	0.276	0.184	0.210
Efficiency	91.5%	73%	11%
$B\eta$	0.0061	0.0016	0.0025
$B\eta$ / $B\eta(\max)$	0.446	0.393	0.076
Q	148.5	442.9	85.6
Q/Q_{LB}	3.18	3.66	0.73

the value of 3 derived by Chu, which is due to the low efficiency of the design. The value of $B\eta/B\eta(\max)$ provides an important comparison among the three designs, where the value of the proposed design is roughly one-fifth that achieved in [4] and [7]. The main parameters that affect the efficiency are the conductive losses in the copper traces and the dielectric losses in the supporting substrate. These are both increased by the fact that the antenna is electrically small, and thus has a high intrinsic Q. Any material losses are effectively multiplied by the Q of the structure, leading to an overall efficiency that is low when the antenna is designed to be electrically small. Our simulations confirm that when the conductive losses are included in the simulation, the efficiency of the antenna is drastically reduced. Additionally, the simplified structure proposed in this letter does not use a spherical volume as efficiently as the works to which it is being compared. A more comprehensive comparison might include fabrication difficulty and cost of materials, which should be reduced in the case of the DPWC design.

V. CONCLUSION

A DPWC antenna is presented to approach the performance of electrically small SSR antennas while utilizing industry standard process in its fabrication. This structure was modeled and optimized using HFSS, and a prototype was fabricated and measured, yielding results comparable to simulation. The measured design approaches the $B\eta/B\eta(\max)$ value achieved in the SSR design, but falls short due to the geometric limitations of a quasi-two-dimensional substrate suspended above a ground plane. However, the proposed structure has fabrication advantages when compared to the spherical split ring design, which makes it a better candidate for large-scale production.

ACKNOWLEDGMENT

The authors would like to thank R. Quarfoth for his assistance with calibration and measurement.

REFERENCES

[1] H. A. Wheeler, "Fundamental limitations of small antennas," *Proc. IRE*, vol. 35, no. 12, pp. 1479–1484, Dec. 1947.
[2] L. J. Chu, "Physical limitations of omni-directional antennas," *J. Appl. Phys.*, vol. 19, no. 12, pp. 1163–1175, 1948.
[3] D. F. Sievenpiper *et al.*, "Experimental validation of performance limits and design guidelines for small antennas," *IEEE Trans. Antennas Propag.*, vol. 60, no. 1, pp. 8–19, Jan. 2012.
[4] O. S. Kim, "Low-Q electrically small spherical magnetic dipole antennas," *IEEE Trans. Antennas Propag.*, vol. 58, no. 7, pp. 2210–2217, Jul. 2010.
[5] O. S. Kim, O. Breinbjerg, and A. D. Yaghjian, "Electrically small magnetic dipole antennas with quality factors approaching the Chu lower bound," *IEEE Trans. Antennas Propag.*, vol. 58, no. 6, pp. 1898–1906, Jun. 2010.
[6] H. L. Thal, "New radiation Q limits for spherical wire antennas," *IEEE Trans. Antennas Propag.*, vol. 54, no. 10, pp. 2757–2763, Oct. 2006.
[7] S. R. Best, "A low Q electrically small magnetic (TE mode) dipole," *IEEE Antennas Wireless Propag. Lett.*, vol. 8, pp. 572–575, 2009.
[8] O. S. Kim and O. Breinbjerg, "Miniaturised self-resonant split-ring resonator antenna," *Electron. Lett.*, vol. 45, no. 4, pp. 196–197, Feb. 2009.
[9] R. M. Fano, L. J. Chu, and R. B. Adler, *Electromagnetic Fields, Energy and Forces*. New York, NY, USA: Wiley, 1960.
[10] S. R. Best, "The radiation properties of electrically small folded spherical helix antennas," *IEEE Trans. Antennas Propag.*, vol. 52, no. 4, pp. 953–960, Apr. 2004.
[11] S. R. Best, "Low Q electrically small linear and elliptical polarized spherical dipole antennas," *IEEE Trans. Antennas Propag.*, vol. 53, no. 3, pp. 1047–1053, Mar. 2005.